Letter

Transmission of vortex electrons through a solenoid

G. K. Sizykh,* A. D. Chaikovskaia, D. V. Grosman, I. I. Pavlov, and D. V. Karlovets†
School of Physics and Engineering, ITMO University, 197101 St. Petersburg, Russia

(Received 24 June 2023; accepted 11 March 2024; published 1 April 2024)

We argue that it is nonstationary Laguerre-Gaussian (NSLG) states rather than the Landau ones that appropriately describe electrons with orbital angular momentum both in their dynamics at the boundary between a solenoid and vacuum and inside the magnetic field. It is shown that the root mean square (rms) radius of the NSLG state oscillates in time and its period-averaged value can significantly exceed the rms radius of the stationary Landau state. We propose several experimental scenarios to probe this unconventional quantum dynamics in the magnetic fields typical for electron microscopes and particle accelerators.

DOI: 10.1103/PhysRevA.109.L040201

Introduction. The manipulation of electrons with orbital angular momentum (OAM), dubbed twisted or vortex electrons [1,2], is a useful tool with great prospects for applications in electron microscopy, nanomaterials studies, particle physics, accelerator physics, and other fields [3–8]. The most common technique to generate twisted electrons is to let the beam go through a phase plate [9,10] or a hologram [3,11,12], alongside methods using surface plasmon polaritons [13]. The states obtained with these methods can often be described as Laguerre-Gaussian wave packets [1,8]. The probability density of such states evolves in time, and a solenoid (magnetic lens) can be used to effectively control the spreading of the packets, both in an electron microscope [14,15] and in a particle accelerator [16].

Within the hard-edge approximation, a thick magnetic lens can be described as a semi-infinite magnetic field. In a real-life experiment (see Fig. 1), a free electron first propagates in vacuum towards the solenoid while spreading, then enters the lens, and continues its propagation inside it. A common description of the transmission of an electron from the field-free space to the solenoid relies on evaluating the dynamics of the observables via the Heisenberg equation of motion, and so no assumptions regarding the electron state are needed. However, far from the boundary the electron state is conventionally thought of as a stationary Landau state [8,17,18] that does not spread in time. There have been several approaches to extend the description of an electron in the field beyond the Landau states [8,19–24]. Nonetheless, the transformation of the electron state itself during the transmission process has not yet been fully understood.

The aim of the present Letter is to point out that it is the *nonstationary Laguerre-Gaussian* (NSLG) states rather than the Landau ones that provide an accurate description of an electron inside a solenoid after passing the boundary. Moreover, we show that the relevance of employing the NSLG states is not only in gaining a consistent description of the electron dynamics near the boundary, but also in predicting the oscillations of the rms radius far from it. In particular, we demonstrate that the time-averaged rms radius of the NSLG state inside the field usually significantly exceeds that of the Landau state, even far away from the boundary where the Landau state might be expected to provide an adequate description. This increase in the rms radius is somewhat analogous to broadening of the classical trajectories during synchrotron radiation [25], but it occurs even when no photons are emitted.

For simplicity, we illustrate our approach with a spinless electron, the transverse energy of which stays much less than mc^2. In principle, spin can easily be included [23], and our approach can be extended into the relativistic regime via the light-cone variables [22,26–28]. Throughout this Letter, $\hbar = c = 1$, the electron charge $e < 0$, and the electron mass equals the inverse Compton wavelength, $m = \lambda_C^{-1}$.

Landau states approach. We introduce the magnetic lens as a semi-infinite stationary and homogeneous magnetic field $\boldsymbol{H} = H\theta(z - z_0)\boldsymbol{e}_z$, $\boldsymbol{e}_z = (0, 0, 1)$. The step function $\theta(z)$ reflects the hard-edge boundary of the lens located at z_0.

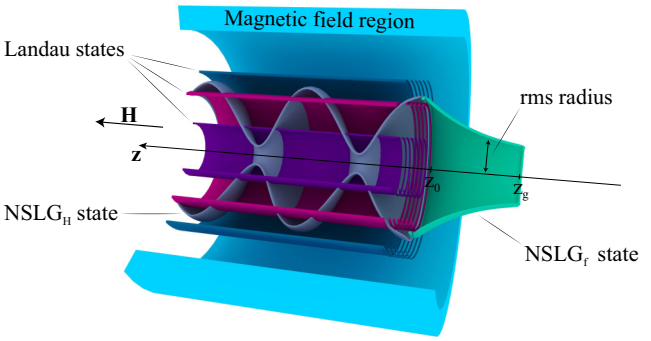

FIG. 1. A free electron passing the boundary between vacuum and a solenoid (magnetic lens). Here, z_g and z_0 are the coordinates of the electron source and the boundary, respectively.

*georgii.sizykh@metalab.ifmo.ru
†dmitry.karlovets@metalab.ifmo.ru

Detailed comments on the whole-space wave function in such an external field, its continuity, and on the applicability of the hard-edge approximation are given in the Supplemental Material [29] (see also Refs. [30,31] therein). The electron wave packet propagates rectilinearly along the z axis with the mean velocity v. To characterize the transverse dynamics of the packet, we study the dynamics of the rms transverse radius $\rho(t) = \sqrt{\langle \rho^2 \rangle (t)}$.

The wave packet generated in free space at a time t_g is known to spread in time according to

$$\rho_\mathrm{f}(t) = \rho_\mathrm{w} \sqrt{1 + (t - t_\mathrm{g})^2 / \tau_\mathrm{d}^2}, \tag{1}$$

where $\tau_\mathrm{d} = \rho_\mathrm{w}/u$ is the diffraction time, ρ_w is the beam waist, u is the transverse velocity dispersion, and the subscript "f" stands for "free" [8]. As such an electron travels from the source to the lens, it acquires a nonzero divergence rate $\rho_0' = d\rho_\mathrm{f}/dt|_{t=t_0}$ and its rms radius grows by a factor of $\rho_0/\rho_\mathrm{w} = \sqrt{1 + (t_0 - t_\mathrm{g})^2/\tau_\mathrm{d}^2}$, where $t_0 = |z_0 - z_\mathrm{g}|/v$ is the moment the electron enters the lens.

Inside the field, the system is described by the Hamiltonian

$$\hat{\mathcal{H}} = -\frac{\lambda_\mathrm{C}}{2}\Delta + \frac{\omega}{2}\hat{L}_z + \frac{\omega^2}{8\lambda_\mathrm{C}}\rho^2 = \hat{\mathcal{H}}_\perp - \frac{\lambda_\mathrm{C}}{2}\partial_z^2, \tag{2}$$

where $\lambda_\mathrm{C} = m^{-1}$ is the Compton wavelength, and $\hat{L}_z = -i\partial/\partial\varphi$ is the canonical OAM operator. The rms radius of the electron starts oscillating according to the Heisenberg equation of motion [8,17,32],

$$\begin{aligned} \rho^2(t) &= \rho_\mathrm{st}^2 + \left(\rho_0^2 - \rho_\mathrm{st}^2\right)\cos(\omega\tau) + \frac{2\rho_0\rho_0'}{\omega}\sin(\omega\tau), \\ \rho_\mathrm{st}^2 &= 2\lambda_\mathrm{C}\omega^{-1}(2\omega^{-1}\langle\hat{\mathcal{H}}_\perp\rangle + \langle\hat{L}_z\rangle). \end{aligned} \tag{3}$$

Here, $\omega = eH\lambda_\mathrm{C}$ is the cyclotron frequency and $\tau = t - t_0 > 0$. The subscript in ρ_st implies the "stationary" radius; the quantity itself is the square root of the period-averaged mean-square radius and is the characteristic radius around which the oscillations occur.

Both in vacuum (1) and inside the lens (3) the expressions for the rms radii can be obtained without specifying the electron state. Nonetheless, the latter quantitatively affects the oscillations of the rms radius by dictating ρ_st^2 in Eq. (3), as well as ρ_w and τ_d in Eq. (1). Far from the boundary, electrons are usually believed to be described by the Landau states, and ρ_st^2 is commonly evaluated with the aid of the Landau wave functions as

$$\rho_\mathrm{st}^2\big|_\mathrm{Landau} = \rho_\mathrm{L}^2 = \sigma_\mathrm{L}^2(2n + |l| + 1), \tag{4}$$

where $\sigma_\mathrm{L} = \sqrt{2/|eH|}$ and ρ_L is the rms radius of the Landau state with a radial quantum number $n = 0, 1, 2, \ldots$ and an OAM $l = 0, \pm1, \pm2, \ldots$ [8,17,32].

As we show hereafter, it is generally not the case that $\rho_\mathrm{st} = \rho_\mathrm{L}$. Equation (4) is satisfied only for the specific boundary values ρ_0 and ρ_0', not governed by any physical principle. In experiment, these parameters can vary from these specific values, leading to a significant increase of ρ_st as compared to ρ_L. That affects the main characteristics of the oscillations.

NSLG states. Let us find an alternative to the Landau state that would describe a twisted electron inside a solenoid after entering it from free space with arbitrary parameters ρ_0 and ρ_0' at the boundary. Following the seminal work of Silenko *et al.* [33], we note that the transverse electron wave function admits a general form, both in vacuum ($z < z_0$) and in the magnetic field ($z > z_0$) [8,33]:

$$\begin{aligned} \Psi_{n,l}(\boldsymbol{\rho}, t) = N \frac{\rho^{|l|}}{\sigma^{|l|+1}(t)} L_n^{|l|}\left(\frac{\rho^2}{\sigma^2(t)}\right) \\ \times \exp\left[il\varphi - i\Phi_\mathrm{G}(t) - \frac{\rho^2}{2\sigma^2(t)}\left(1 - i\frac{\sigma^2(t)}{\lambda_\mathrm{C} R(t)}\right)\right]. \end{aligned} \tag{5}$$

We refer to it as a *nonstationary Laguerre-Gaussian* state. The wave function (5) describes a vortex electron with an OAM l, and the difference between the NSLG states in free space ($\mathrm{NSLG_f}$) and in the magnetic field ($\mathrm{NSLG_H}$) is governed by the optical functions: dispersion $\sigma(t)$, radius of curvature $R(t)$, and Gouy phase $\Phi_\mathrm{G}(t)$.

The rms radius of the NSLG state is

$$\rho(t) = \sigma(t)\sqrt{2n + |l| + 1}. \tag{6}$$

Equations for the optical functions of the $\mathrm{NSLG_H}$ state follow from the Schrödinger equation:

$$\begin{aligned} &\frac{1}{R(t)} = \frac{\sigma'(t)}{\sigma(t)}, \\ &\frac{1}{\lambda_\mathrm{C}^2 R^2(t)} + \frac{1}{\lambda_\mathrm{C}^2}\left[\frac{1}{R(t)}\right]' = \frac{1}{\sigma^4(t)} - \frac{1}{\sigma_\mathrm{L}^4}, \\ &\frac{1}{\lambda_\mathrm{C}}\Phi_\mathrm{G}'(t) = \frac{l}{\sigma_\mathrm{L}^2} + \frac{(2n + |l| + 1)}{\sigma^2(t)}. \end{aligned} \tag{7}$$

The first equation in (7) allows us to further use $\sigma'(t)$ rather than $R(t)$ as a characteristic of the NSLG packet.

A special choice of the initial conditions $\sigma(t_0) = \sigma_\mathrm{L}$, $\sigma'(t_0) = 0$ for the system (7) leads to a nonspreading solution

$$\sigma(t) = \sigma_\mathrm{L}, \quad \sigma'(t) = 0, \quad \Phi_\mathrm{G}(t) = \varepsilon_\perp t, \tag{8}$$

where $\varepsilon_\perp = \omega(2n + |l| + l + 1)/2$ is the energy of the Landau state. These optical functions turn the state (5) exactly into the Landau one with ρ_st given by Eq. (4).

To find the more general form of the $\mathrm{NSLG_H}$ state, we suggest solving the system (7) with initial conditions for the dispersion and its derivative given by the $\mathrm{NSLG_f}$ state at the time t_0 when the electron enters the lens,

$$\begin{aligned} \sigma(t_0) = \sigma_0 = \frac{\rho_0}{\sqrt{2n + |l| + 1}}, \\ \sigma'(t_0) = \sigma_0' = \frac{\rho_0'}{\sqrt{2n + |l| + 1}}, \end{aligned} \tag{9}$$

where ρ_0 and ρ_0' are the rms radius (1) and the divergence rate of the $\mathrm{NSLG_f}$ state generated in field-free space at the time t_g, respectively. These conditions imply the continuity of the wave function at the boundary. We abstain from writing down the Gouy phase because it does not affect the dynamics of the rms radius.

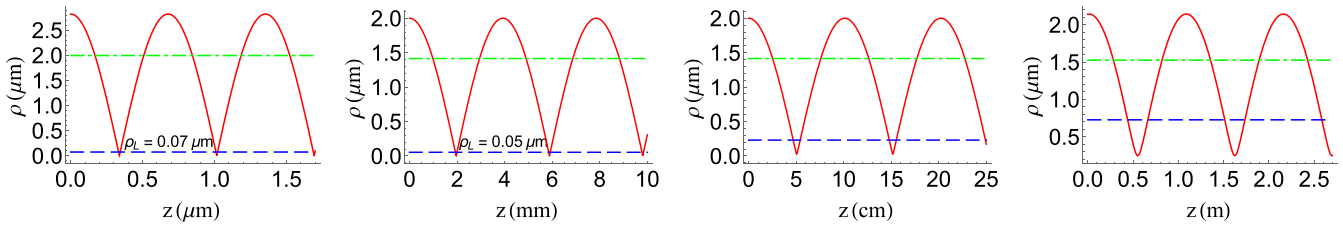

FIG. 2. Oscillations of the rms radius of the $\mathrm{NSLG_H}$ wave packet in a magnetic field (solid red line), $\rho_{\mathrm{st}} = (1/T_{\mathrm{c}}) \int_0^{T_{\mathrm{c}}} \rho^2(t)dt$ (dotted-dashed green line) and ρ_{L}(dashed blue line). The parameters are listed in Table I. (a) SEM, (b) TEM, (c) medical linac, (d) conventional linac.

The dispersion of the $\mathrm{NSLG_H}$ packet then reads

$$\sigma(t) = \sigma_{\mathrm{st}} \sqrt{1 + \sqrt{1 - \left(\frac{\sigma_{\mathrm{L}}}{\sigma_{\mathrm{st}}}\right)^4}\, \sin\left[s(\sigma_0, \sigma_0')\omega(t - t_0) - \theta\right]},$$
$$\sigma_{\mathrm{st}}^2 = \frac{\sigma_0^2}{2}\left[1 + \left(\frac{\sigma_{\mathrm{L}}}{\sigma_0}\right)^4 + \left(\frac{\sigma_0'\sigma_{\mathrm{L}}^2}{\lambda_{\mathrm{C}}\sigma_0}\right)^2\right], \tag{10}$$
$$\theta = \arcsin \frac{1 - (\sigma_0/\sigma_{\mathrm{st}})^2}{\sqrt{1 - (\sigma_{\mathrm{L}}/\sigma_{\mathrm{st}})^4}},$$

where we have defined

$$s(\sigma_0, \sigma_0') = \begin{cases} \mathrm{sgn}(\sigma_0'), & \sigma_0' \neq 0, \\ \mathrm{sgn}(\sigma_{\mathrm{L}} - \sigma_0), & \sigma_0' = 0, \\ 0, & \sigma_0 = \sigma_{\mathrm{L}} \text{ and } \sigma_0' = 0. \end{cases} \tag{11}$$

Notice that the quantum numbers n and l do not affect the rms radius dynamics, except for scaling the oscillation magnitudes according to Eq. (6). Thus, even if a Gaussian electron with $n = l = 0$ approaches the magnetic field, the same conditions $\sigma(t_0) = \sigma_{\mathrm{L}}$, $\sigma'(t_0) = 0$ have to hold for the electron to turn into the Landau electron inside the field.

An $\mathrm{NSLG_H}$ state may be thought of as a complex superposition of a large number of Landau states [34]. However, it is still possible to obtain a single Landau state in a solenoid. This can be achieved by refocusing the electron beam so that its waist is at the boundary and adjusting the beam size and the field strength, ensuring $\sigma_0 = \sigma_{\mathrm{L}}$, which can be somewhat challenging to realize in experiment.

One can give the following qualitative explanation for the oscillations of the rms radius according to Eq. (10) involving two processes. First, the wave packet shrinks because of the Lorentz force acting on each Bohmian trajectory. Second, the wave packet spreads similar to an $\mathrm{NSLG_f}$ in Eq. (1). While the wave packet is wide, the radial Lorentz force, caused by the azimuthal velocity component in the longitudinal magnetic field, dominates, leading to a decrease in the rms radius. As the radius becomes small enough, the quantum-mechanical spreading of the wave packet takes over and leads to expansion instead of shrinking.

The mean energy of the $\mathrm{NSLG_H}$ state,

$$\langle E_\perp \rangle = \frac{\omega}{2}(2n + |l| + 1)\frac{\sigma_{\mathrm{st}}^2}{\sigma_{\mathrm{L}}^2} + \frac{\omega}{2} l \geqslant \varepsilon_\perp, \tag{12}$$

is almost always greater than the energy of the Landau state because $\sigma_{\mathrm{st}}^2/\sigma_{\mathrm{L}}^2 \geqslant 1$. The resulting energy excess can be attributed to the intrinsic motion of the wave packet due to the rms radius oscillations. This motion can be interpreted as quantum betatron oscillations [25]. Such an $\mathrm{NSLG_H}$ state's "breathing" is also reflected in a larger scale of the stationary radius ρ_{st}^2, when evaluated with the $\mathrm{NSLG_H}$ state,

$$\rho_{\mathrm{st}}^2\big|_{\mathrm{NSLG_H}} = \frac{1}{T_{\mathrm{c}}}\int_0^{T_{\mathrm{c}}} \rho^2(t)dt = \rho_{\mathrm{L}}^2 \frac{\sigma_{\mathrm{st}}^2}{\sigma_{\mathrm{L}}^2} \geqslant \rho_{\mathrm{L}}^2, \tag{13}$$

where $T_{\mathrm{c}} = 2\pi m/|eH|$ is the cyclotron period. To underline the distinction between the $\mathrm{NSLG_H}$ state and the Landau one we introduce

$$\xi_1 = \frac{\sigma_{\mathrm{L}}}{\sigma_0}, \quad \xi_2 = \frac{|\sigma_0'|\sigma_{\mathrm{L}}}{\lambda_{\mathrm{C}}}. \tag{14}$$

When $\xi_1 = 1$ and $\xi_2 = 0$, ρ_{st}^2 of Eq. (13) coincides with that of Eq. (4), obtained with the Landau state. However, in this case Eq. (3) degenerates into $\rho^2(t) = \rho_{\mathrm{L}}^2$ and no oscillations occur at all. From Eq. (13) it follows that $\rho_{\mathrm{st}}^2|_{\mathrm{NSLG_H}} \gg \rho_{\mathrm{L}}^2$ when either $\xi_1 \gg 1$, $\xi_1 \ll 1$, or $\xi_2 \gg 1$.

To illustrate the current approach, we compare our results with the dynamics of twisted electrons investigated experimentally in Refs. [14,15]. The authors obtained a free-electron state that, after refocusing, enters a region of a quasiuniform magnetic field and shrinks in size while propagating inside it. During the time when the size of the electron wave packet inside the solenoid stays comparable to ρ_{L}, the electron is thought of as a Landau state. However, the process of the electron crossing the boundary between vacuum and magnetic field and further propagating inside might be better interpreted in the NSLG states formalism. One can reproduce the obtained behavior of the rms radius inside the lens [see Fig. 2(b) in Ref. [14]] using Eqs. (10) and (6) and the parameters $n = 0$, $|l| = 1$, $\sigma_0 = 4.77 \times 10^{-2}$ μm, $\sigma_0' = -3.1 \times 10^{-4}$. Thus, we argue that what was observed in Ref. [14] may be a part of the oscillations predicted by the NSLG states approach. For the discussed experimental setup we estimate that $\xi_1 = 0.76$ and $\xi_2 = 29.21 \gg 1$ leading to

$$\rho_{\mathrm{st}}^2\big|_{\mathrm{NSLG_H}} = 20.7\, \rho_{\mathrm{L}} \gg \rho_{\mathrm{L}}. \tag{15}$$

Hence, typically, ρ_{st} significantly exceeds ρ_{L} and for oscillations to occur around the latter *very specific* parameters of the incoming electron packet must align.

Experimental feasibility. To observe the oscillations of the rms radius described by the $\mathrm{NSLG_H}$ state, we propose

TABLE I. Experimental scenarios for observing the oscillations of the rms radius $\rho(z)$. We take $\sigma_w = 1$ μm, $n = 0$, $l = 3$. The parameters $\xi_1 = \sigma_L/\sigma_0$ and $\xi_2 = \sigma_0'\sigma_L^2/(\lambda_C\sigma_0)$ reflect the discrepancy between the $\mathrm{NSLG_H}$ state and the Landau one, the latter being reproduced when $\xi_1 = 1$ and $\xi_2 = 0$.

Setup	$E_\parallel$	v	H	ρ_L	d	z_R	ρ_0	$d\rho/dz\|_{z=z_0}$	ξ_1	ξ_2
SEM	1 keV	0.06 c	1 T	72.6 nm	16.3 cm	16.3 cm	2.82 μm	8.7 pm/μm	0.026	6.7×10^{-4}
TEM	200 keV	0.70c	1.9 T	52.7 nm	10 cm	179 cm	2 μm	62 pm/mm	0.026	3.9×10^{-5}
Medical linac	1 MeV	0.94c	0.1 T	0.23 μm	10 cm	243 cm	2 μm	0.34 nm/cm	0.115	5.5×10^{-4}
Linac	1 GeV	c	0.01 T	0.72 μm	100 cm	258 cm	2.14 μm	0.28 μm/m	0.339	0.045

several experimental scenarios for the parameters and energy scales typical for different setups: a scanning electron microscope (SEM), a transmission electron microscope (TEM), a low-energy linear accelerator (for instance, for medical applications), and a conventional linac. Additional solenoids must be adjusted to these electron sources to provide regions of approximately constant and homogeneous magnetic field. In an experiment, the distribution of a twisted electron probability density in the transverse plane can be measured consecutively at various distances z along the solenoid axis with, for instance, a CCD camera. Subsequently, $\sqrt{\langle\rho^2\rangle}$, obtained as a function of z, can be expressed in terms of $t = z/v$ and compared to our predictions.

The parameters for different setups are presented in Table I and the corresponding oscillations of the rms radii are depicted in Fig. 2. We take $\sigma_w = 1$ μm (a characteristic scale [3,9,11] for the devices generating twisted electrons) and consider quantum numbers $n = 0$, $l = 3$, that result in $\rho_w = 2$ μm. A different choice of the quantum numbers would lead to simple rescaling of the rms radius according to Eq. (6).

In Table I we also use the longitudinal energy $E_\parallel$, magnetic field strength H, and the distance between the source of twisted electrons and the magnetic field d that are typical for the proposed experimental scenarios [35]. For SEM, we take a particular value $d = 16.3$ cm for calculation convenience, though any distance of the order of several cm is appropriate. We adjust the magnetic field strength in order to observe several oscillation periods at realistic distances for each setup. For instance, for a linac we take $H = 0.01$ T in order to observe oscillations at several meters. If needed, one may increase the field strength to proportionally decrease the observation distance. On the other hand, SEM and TEM usually have magnetic fields of the order of 1 T and their observation distances are somewhat limited by their design.

For the $\mathrm{NSLG_f}$ state with $\sigma_w = 1$ μm, the diffraction time is $\tau_d = \sigma_w^2/\lambda_C = 8.6$ ns, and the Rayleigh length, $z_R = v\tau_d$, scales with the electron energy. For example, in the second row of Table I, the Rayleigh length for TEM, $z_R = 179$ cm, is much greater than the distance between the source and the solenoid, $d = 10$ cm. This leads to the rms radius at the boundary $\rho_0 \approx 2$ μm being almost the same as that at the electron source $\rho_w = 2$ μm. The divergence rate $d\rho/dz|_{z=z_0} = \rho_0'/v$ reflects the change in the rms radius with the distance traveled by the electron along the field near the boundary. For the proposed scenarios, ξ_2, the dimensionless analog of the divergence rate, shows that the divergence rate is low and does not affect the dynamics of the electron in solenoids.

Notice the sharp wedgelike pattern of the rms radius oscillations in the bottom parts of Figs. 2(a)–2(c). It illustrates the influence of the parameters ξ_1 and ξ_2 on the electron behavior inside the field. Deviations of ξ_1 from 1 and ξ_2 from 0 in all the entries of Table I emphasize the distinction between the $\mathrm{NSLG_H}$ state and the Landau one. For SEM, TEM, and a medical linac, ρ_{st} (dotted-dashed green line in Fig. 2) is almost an order of magnitude greater than ρ_L (dashed blue line). On the other hand, for a linac [Fig. 2(d)] the parameters ξ_1 and ξ_2 do not differ as much from 1 and 0, correspondingly, and ρ_{st} is just twice larger than ρ_L.

Conclusion. We have put forward an approach to the problem of transmission of a free twisted electron through a sharp boundary between a solenoid and vacuum based on the description in terms of NSLG states. This formalism enables the smooth transition of a free $\mathrm{NSLG_f}$ state to a single $\mathrm{NSLG_H}$ mode inside the field. The transformation of a free Laguerre-Gaussian electron inside the lens into the $\mathrm{NSLG_H}$ state leads to oscillations of the rms radius. These oscillations have usually been expected to occur around the value predicted by the stationary Landau state. Somewhat counterintuitively, the time-averaged value of the rms radius can generally be much larger (up to several orders of magnitude) than ρ_L. For instance, for typical TEM parameters $H = 1.9$ T, $\sigma_0 = 47.7$ nm, $\sigma_0' = -3.1\times10^{-4}$ from Ref. [14], ρ_{st} is 20 times larger than the one predicted by the Landau states. The opposite case is $\sigma_0 \simeq \sigma_L$ and $\sigma_0' \ll \lambda_C/\sigma_L$. For such parameters, the $\mathrm{NSLG_H}$ states resemble the Landau ones and the oscillations occur around ρ_L with a low magnitude.

Although there is evidence that the $\mathrm{NSLG_H}$ states more adequately describe quantum dynamics of the vortex electrons inside a magnetic lens, further experimental as well as theoretical scrutiny is required. For example, going beyond the hard-edge approximation, and considering an off-axis entering of an electron into a solenoid would make the proposed approach more realistic. We have proposed several scenarios that have the potential to observe the rms radius oscillations with parameters typical for setups ranging from SEM to linear accelerators.

Acknowledgments. We are grateful to N. Sheremet, V. Ivanov, and S. Baturin for offering their opinion on the draft. The work is funded by Russian Science Foundation and St. Petersburg Science Foundation, Project No. 22-22-20062 [36].

[1] K. Y. Bliokh, I. P. Ivanov, G. Guzzinati, L. Clark, R. Van Boxem, A. Béché, R. Juchtmans, M. A. Alonso, P. Schattschneider, F. Nori, and J. Verbeeck, Theory and applications of free-electron vortex states, Phys. Rep. **690**, 1 (2017).

[2] S. Lloyd, M. Babiker, G. Thirunavukkarasu, and J. Yuan, Electron vortices: Beams with orbital angular momentum, Rev. Mod. Phys. **89**, 035004 (2017).

[3] J. Verbeeck, H. Tian, and P. Schattschneider, Production and application of electron vortex beams, Nature (London) **467**, 301 (2010).

[4] J. C. Idrobo and S. J. Pennycook, Vortex beams for atomic resolution dichroism, Microscopy **60**, 295 (2011).

[5] Z. Mohammadi, C. P. Van Vlack, S. Hughes, J. Bornemann, and R. Gordon, Vortex electron energy loss spectroscopy for near-field mapping of magnetic plasmons, Opt. Express **20**, 15024 (2012).

[6] V. Grillo, T. R. Harvey, F. Venturi, J. S. Pierce, R. Balboni, F. Bouchard, G. C. Gazzadi, S. Frabboni, A. H. Tavabi, Z.-A. Li, R. E. Dunin-Borkowski, R. W. Boyd, B. J. McMorran, and E. Karimi, Observation of nanoscale magnetic fields using twisted electron beams, Nat. Commun. **8**, 689 (2017).

[7] I. P. Ivanov, Promises and challenges of high-energy vortex states collisions, Prog. Part. Nucl. Phys. **127**, 103987 (2022).

[8] D. Karlovets, Vortex particles in axially symmetric fields and applications of the quantum Busch theorem, New J. Phys. **23**, 033048 (2021).

[9] M. Uchida and A. Tonomura, Generation of electron beams carrying orbital angular momentum, Nature (London) **464**, 737 (2010).

[10] P. Schattschneider, M. Stöger-Pollach, and J. Verbeeck, Novel vortex generator and mode converter for electron beams, Phys. Rev. Lett. **109**, 084801 (2012).

[11] B. J. McMorran, A. Agrawal, I. M. Anderson, A. A. Herzing, H. J. Lezec, J. J. McClelland, and J. Unguris, Electron vortex beams with high quanta of orbital angular momentum, Science **331**, 192 (2011).

[12] V. Grillo, E. Karimi, G. C. Gazzadi, S. Frabboni, M. R. Dennis, and R. W. Boyd, Generation of nondiffracting electron Bessel beams, Phys. Rev. X **4**, 011013 (2014).

[13] G. M. Vanacore, G. Berruto, I. Madan, E. Pomarico, P. Biagioni, R. J. Lamb, D. McGrouther, O. Reinhardt, I. Kaminer, B. Barwick, H. Larocque, V. Grillo, E. Karimi, F. J. G. de Abajo, and F. Carbone, Ultrafast generation and control of an electron vortex beam via chiral plasmonic near fields, Nat. Mater. **18**, 573 (2019).

[14] P. Schattschneider, Th. Schachinger, M. Stöger-Pollach, S. Löffler, A. Steiger-Thirsfeld, K. Y. Bliokh, and F. Nori, Imaging the dynamics of free-electron Landau states, Nat. Commun. **5**, 4586 (2014).

[15] T. Schachinger, S. Löffler, M. Stöger-Pollach, and P. Schattschneider, Peculiar rotation of electron vortex beams, Ultramicroscopy **158**, 17 (2015).

[16] M. Reiser, *Theory and Design of Charged Particle Beams* (Wiley, New York, 2008).

[17] C. R. Greenshields, R. L. Stamps, S. Franke-Arnold, and S. M. Barnett, Is the angular momentum of an electron conserved in a uniform magnetic field? Phys. Rev. Lett. **113**, 240404 (2014).

[18] C. R. Greenshields, S. Franke-Arnold, and R. L. Stamps, Parallel axis theorem for free-space electron wavefunctions, New J. Phys. **17**, 093015 (2015).

[19] V. G. Bagrov, M. C. Baldiotti, D. M. Gitman, and I. V. Shirokov, New solutions of relativistic wave equations in magnetic fields and longitudinal fields, J. Math. Phys. **43**, 2284 (2002).

[20] K. Y. Bliokh, P. Schattschneider, J. Verbeeck, and F. Nori, Electron vortex beams in a magnetic field: A new twist on Landau levels and Aharonov-Bohm states, Phys. Rev. X **2**, 041011 (2012).

[21] G. M. Gallatin and B. McMorran, Propagation of vortex electron wave functions in a magnetic field, Phys. Rev. A **86**, 012701 (2012).

[22] V. G. Bagrov and D. M. Gitman, *The Dirac Equation and Its Solutions* (de Gruyter, Berlin, 2014).

[23] L. Zou, Z. Pengming, and A. J. Silenko, General quantum-mechanical solution for twisted electrons in a uniform magnetic field, Phys. Rev. A **103**, L010201 (2021).

[24] A. Melkani and S. J. van Enk, Electron vortex beams in nonuniform magnetic fields, Phys. Rev. Res. **3**, 033060 (2021).

[25] A. A. Sokolov and I. M. Ternov, *Radiation from Relativistic Electrons* (American Institute of Physics, Woodbury, NY, 1986).

[26] D. Karlovets, Gaussian and Airy wave packets of massive particles with orbital angular momentum, Phys. Rev. A **91**, 013847 (2015).

[27] R. Ducharme, I. G. da Paz, and A. G. Hayrapetyan, Fractional angular momenta, Gouy and Berry phases in relativistic Bateman-Hillion-Gaussian beams of electrons, Phys. Rev. Lett. **126**, 134803 (2021).

[28] U. D. Jentschura, Algebraic approach to relativistic Landau levels in the symmetric gauge, Phys. Rev. D **108**, 016016 (2023).

[29] See Supplemental Material at http://link.aps.org/supplemental/10.1103/PhysRevA.109.L040201 for comments on the whole-space wave function (Sec. I), a demonstration of the continuity of the wave function implied (Sec. II), and a discussion of the applicability of the hard-edge approximation (Sec. III).

[30] R. Lefebvre, Continuity conditions for a time-dependent wavefunction, J. Mol. Struct. (THEOCHEM) **493**, 117 (1999).

[31] H. Wollnik, *Optics of Charged Particles* (Academic Press, London, 1987).

[32] S. Baturin, D. Grosman, G. K. Sizykh, and D. V. Karlovets, Evolution of an accelerated charged vortex particle in an inhomogeneous magnetic lens, Phys. Rev. A **106**, 042211 (2022).

[33] L. Zou, P. Zhang, and A. J. Silenko, Production of twisted particles in magnetic fields, J. Phys. B: At. Mol. Opt. Phys. **57**, 045401 (2024).

[34] G. K. Sizykh, A. D. Chaikovskaia, D. V. Grosman, I. I. Pavlov, and D. V. Karlovets, Nonstationary Laguerre-Gaussian states vs Landau ones: choose your fighter, arXiv:2309.15899.

[35] H. Wiedemann, *Particle Accelerator Physics* (Springer, Cham, 2015).

[36] https://www.rscf.ru/project/22-22-20062/.